



ELSEVIER

Available at
www.ComputerScienceWeb.com
POWERED BY SCIENCE @ DIRECT®

Performance Evaluation 55 (2004) 165–181

**PERFORMANCE
EVALUATION**
An International
Journal

www.elsevier.com/locate/peva

Modeling frame-level errors in GSM wireless channels

Ping Ji*, Benyuan Liu, Don Towsley, Zihui Ge, Jim Kurose

University of Massachusetts, Computer Science Building, 140 Governors Drive, Amherst, MA 01003, USA

Abstract

We compare four different approaches to modeling frame-level errors in GSM channels. One of these, the Markov-based Trace Analysis (MTA) model, was developed explicitly for this purpose. The next two, k th-order Markov models and hidden Markov models (HMMs), have been widely used to model loss in wired networks. All three of these have difficulty in modeling empirical GSM frame-level error traces. The MTA model and HMM predict frame-error rates substantially different from that measured from the trace, and all three models have difficulty in capturing the long term temporal correlation structure. We propose a fourth model, the extended On/Off model, which alternates between an On (error-free) and an Off (error-filled) state. The state holding times are taken from mixtures of geometric distributions. We show that this model, with mixtures of 4–7 geometric distributions captures first- and second-order statistics significantly better than the preceding three approaches. © 2003 Elsevier B.V. All rights reserved.

Keywords: Markov-based Trace Analysis; On/Off model; Frame-level errors

1. Introduction

There has been substantial recent interest in the development and deployment of wireless data communication systems such as 3G wireless networks, IEEE 802.11, and Bluetooth. The characteristics of such wireless channels (in particular, with respect to frame-level errors) are quite different from those of traditional wired links [8]. Most wireless channel modeling efforts have focused on physical layer properties such as the signal to noise ratio. Communication protocols at the network layer and above, however, operate on the basic unit of a frame (or packet); and the choice of error model matters for the behavior of higher layer protocols [14]. Frame-level wireless channel models are thus of particular interest in the design and evaluation of such protocols in wireless networks.

A recent paper by Konrad et al. [5] proposed and evaluated a frame-level error model for GSM channels. They used a high-order Markov model to capture channel behavior in a so-called *bad state*, and empirically fit exponential distributions to measured data to model the lengths of alternating intervals of time spent in “bad” and “good” states. Their Markov-based Trace Analysis (MTA) model was shown to capture the correlation structure during “bad” periods better than the classical Gilbert model [9]. However, the MTA

* Corresponding author. Tel.: +1-413-545-3179; fax: +1-413-545-1479.

E-mail addresses: jiping@cs.umass.edu (P. Ji), benyuan@cs.umass.edu (B. Liu), towsley@cs.umass.edu (D. Towsley), gezihui@cs.umass.edu (Z. Ge), kurose@cs.umass.edu (J. Kurose).

model is unable to match important statistics such as the frame-error rate (FER) and the autocorrelation function of the frame-level error time series.

In this paper, we consider three alternative approaches towards modeling frame-level errors in GSM channels. Our analysis of the frame-level traces in [5] reveals temporal correlation in the frame-level error process over relatively long time scales, as well as high variability in the distribution of consecutive error-filled and error-free frames, neither of which is captured by the model proposed in [5]. The first two alternative approaches, based on the k th-order Markov chains and hidden Markov models (HMMs), have been used to model wired links. Unfortunately, they do little better than the MTA model to accurately model various first- and second-order statistics, even when they are allowed to have relatively large state spaces. On the other hand, we find that a two-state semi-Markov model (henceforth referred to as an *extended On/Off model*), where the state holding times of one or both states are characterized by mixtures of geometric distributions captures first- and second-order statistics such as FER and autocorrelation function. Furthermore, we find that each mixture needs not more than four geometric distributions, and EM algorithm improves the capability of the extended On/Off model on capturing the FER.

The remainder of this paper is organized as follows. In Section 2, we analyze the GSM channel frame-error trace from [5], study its statistical properties, and identify the characteristics of the frame-error trace that should be captured in a frame-level error model. Section 3 describes the MTA model and two other approaches that have been used to successfully model packet errors in wired links, and their application to modeling GSM channels. Section 4 introduces the schemes of deriving the first- and second-order statistics from a Markov model. Section 5 describes our extended On/Off model in detail. In Section 6, we demonstrate the ability of our extended On/Off model to more accurately capture both first- and second-order statistics of the frame-error process. Section 7 concludes the paper.

2. Modeling GSM channels

We begin by analyzing the GSM channel link-layer frame-error trace gathered by Konrad et al. [5]. In this trace, frame-level wireless communication was recorded for approximately 215 min between a laptop host and a fixed end host. When a frame was received without bit errors, a ‘0’ was recorded, when a corrupted frame was received, a ‘1’ was recorded (regardless of whether the link-layer protocol was able to recover the frame via re-transmission [7,5]). Thus, a binary sequence representing the frame-errors of the GSM channel was generated, see [5] for details.

Fig. 1 shows the FER of this GSM trace smoothed over a window of 10,000 samples. While the entire trace shows large variations over time, we can roughly identify three distinct portions of the trace, as shown in Fig. 1. Parts 1 and 3 each contains approximately 225,000 samples, while part 2 contains about 170,000 samples. Note that the third part of the trace shows a trend of increasing FER.

2.1. Stationarity test

Since our goal is to develop Markov models for stationary loss processes, it is important to identify segments of the trace that are stationary. We study the stationarity of the three trace parts shown in Fig. 1 separately using the *runtest* and the *reverse arrangements test* [1], which perform hypothesis tests on the underlying trend and other variations of random data sequences.

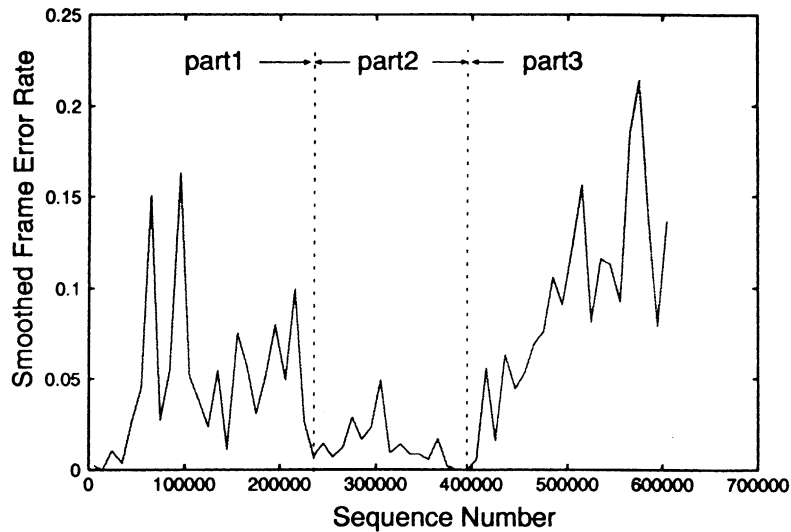


Fig. 1. Smoothed error rate of empirical data with window size 10,000.

To perform the stationarity test, we assume that the GSM frame-level error is a random process $\{Z_i\}_{i=1}^n$, where n is the total number of samples in the sequence, and each sample Z_i takes an value 1 (when a GSM frame is corrupted) or value 0 (when a GSM frame is correct). The stationarity of $\{Z_i\}$ can thus be tested by the steps shown in Fig. 2.

Note that, step 3 of Fig. 2 introduces two approaches, *runtest* and *reverse arrangement test*, that can be used to examine the underlying trends or variations of a random sequence. The *runtest* and the *reverse arrangement test* are hypothesis tests, which assume that there are no underlying trends for the random sequence being tested and uses contradictory conclusions to invalidate the assumption. The details of both stationarity tests can be found in [1].

1. Divide a GSM frame error trace, $\{Z_i\}_{i=1}^n$, into equal length time intervals, each of which contains m samples.
2. Compute a mean value for each time interval and align these sample mean values in a time sequence, $\{Z_i^{(m)}\}$, where $\{Z_i^{(m)}\}$ is an aggregation of $\{Z_i\}$, and $Z_i^{(m)} = \frac{1}{m} \sum_{j=1}^m Z_{(i-1)m+j}$.
3. Test the sequence of mean values, $\{Z_i^{(m)}\}$, for the presence of underlying trends or variations other than those due to expected sampling variations. For examining the underlying trends or variations, we use two approaches: the *runtest* and the *reverse arrangements test*.
4. If there is an underlying trend in the mean values, then the original GSM sample trace is not stationary.

Fig. 2. Procedure of testing the stationarity for a GSM frame-level error trace.

We apply both of the runtest and the reverse arrangements test on the entire GSM trace and on each subtrace of the empirical GSM trace. Basically, each subtrace shown in Fig. 1 is divided into N equal length segments. A sample mean is calculated for each segment, and is used in the stationarity tests. The results of both the runtest and the reverse arrangements test typically depend on the segment length used, and thus we applied these tests to the entire GSM trace, and to the three subtraces separately, using various segment lengths. We found that, at the significance level of 0.02, the entire GSM trace passes the stationarity tests only when the segment size is larger than 50,000 samples. Part 1 passes the stationarity tests when the segment size exceeds 2200 samples, part 2 passes all the stationarity tests with a segment size larger than 800 samples, and part 3 cannot pass the reverse arrangements test because of its significant increasing trend. Given these observations, we chose to study the three trace parts separately, and focus on parts 1 and 2.

2.2. Examine the first- and second-order statistics of GSM trace

We are interested in modeling the behavior of the frame-level errors of GSM channels, and we focus on the following first- and second-order statistics in our analysis.

Let $\{Z_i\}$ denote a wide sense stationary sequence of random variables corresponding to the frame-error trace. Let $\{X_i\}$, $\{Y_i\}$ denote the lengths of error and error-free bursts, respectively, where we define an error burst as a sequence of consecutive corrupted frames (1's), and an error-free burst as a sequence of consecutive correct frames (0's). Furthermore, let X be the random variable of error burst length with mean \bar{X} , and Y be the random variable of error-free burst length with mean \bar{Y} , and let σ_X and σ_Y be the standard deviation of the error and error-free burst lengths, respectively:

- *FER*. The FER is given by \bar{Z} .
- *Coefficient of variation (CoV)*. The CoVs of the error and error-free burst lengths are

$$\text{Cov}(X) = \frac{\sigma_X}{\bar{X}}, \quad (1)$$

$$\text{Cov}(Y) = \frac{\sigma_Y}{\bar{Y}}. \quad (2)$$

- *Complementary cumulative distribution function (CCDF)*. The CCDF of X and Y are defined as

$$F_X^{(c)}(x) = P\{X > x\}, \quad (3)$$

$$F_Y^{(c)}(y) = P\{Y > y\}. \quad (4)$$

- *Autocorrelation*. The autocorrelation function of a frame-error trace is defined as

$$\rho_Z(h) = \frac{E[(Z_{i+h} - \bar{Z})(Z_i - \bar{Z})]}{E[(Z_i - \bar{Z})^2]}, \quad (5)$$

where h is the lag and \bar{Z} the sample mean of Z .

For each of the three GSM trace parts, we calculated its FER and the CoVs of the error and error-free burst lengths. The resulting FER and CoVs are shown in Table 1. From Table 1, we observe that $\text{CoV}(X)$ and $\text{CoV}(Y)$ of the three trace parts are greater than 1, implying that the burst lengths demonstrate higher variability than that of a geometric distribution (which has a CoV less than or equal to 1).

Table 1
FER and CoV for error and error-free bursts

	FER	CoV of burst length	
		Error burst	Error-free burst
Part 1	0.0503	2.064	5.116
Part 2	0.0134	1.087	3.452
Part 3	0.0799	2.850	5.875

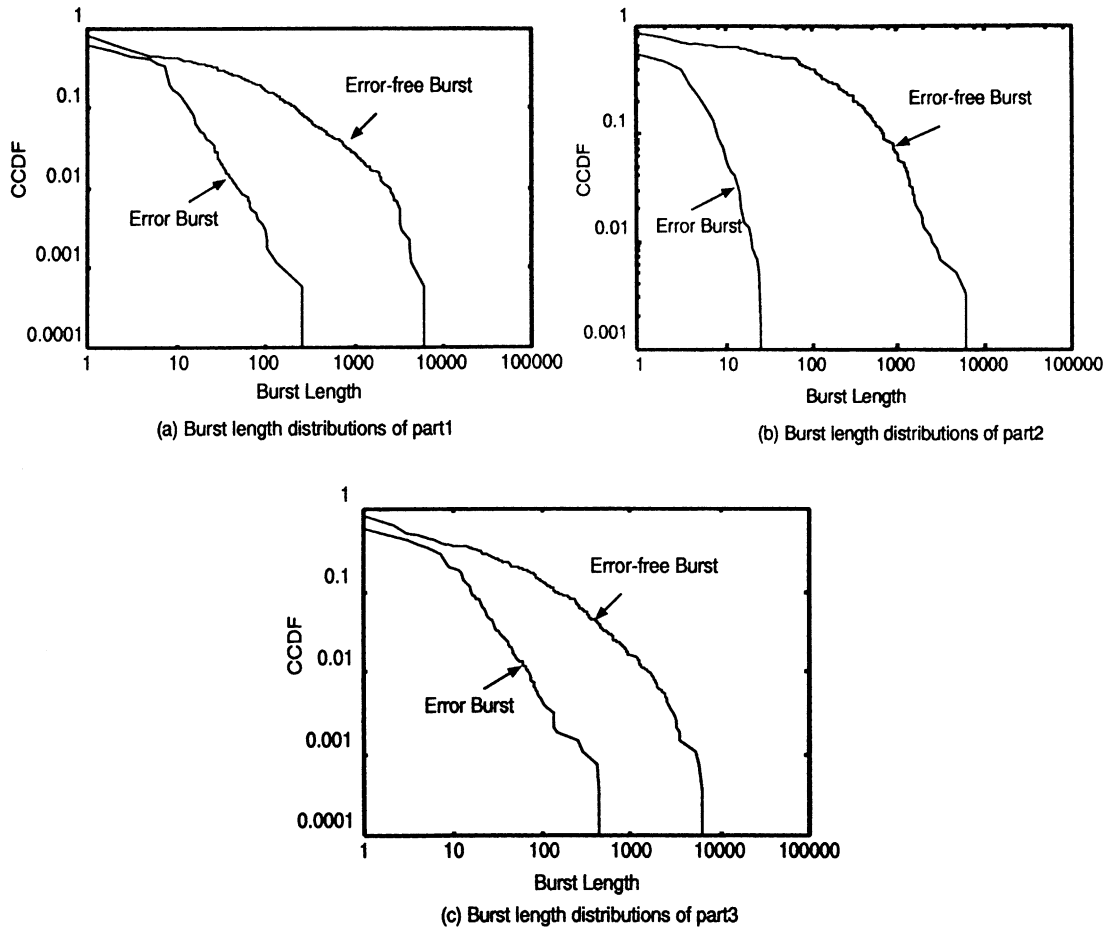


Fig. 3. The CCDFs of the three parts of GSM empirical trace.

In addition, Fig. 3 shows the CCDFs of the error and error-free burst lengths of the three GSM trace parts, and Fig. 4 shows their autocorrelation functions with the confidence bounds of significance level 0.05 shown as the dashed lines.¹ From the above first- and second-order statistics of the empirical traces, we observe that the GSM frame-level error trace exhibits high loss and high variability. We would like to

¹ For details of the calculation of confidence bounds, see [2].

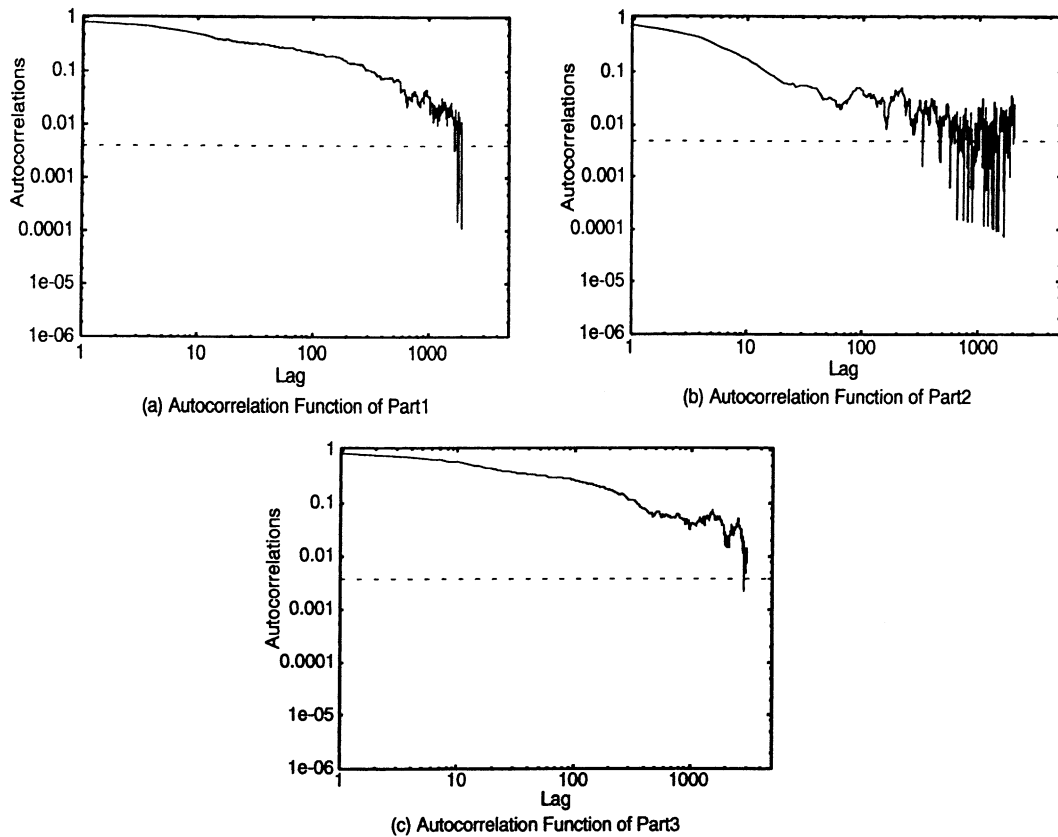


Fig. 4. The autocorrelation functions of the first and the second parts of GSM empirical trace.

build models to capture such behaviors of the first- and second-order statistics of the GSM channels. To do that, we first examine several Markovian based models.

3. Three models for predicting frame-error performance measures

As noted in Section 1, a recent paper by Konrad et al. [5] proposed and evaluated a model for frame-level errors in GSM channels. In this section, we review this model, as well as two other models— k th-order Markov model and HMM—that have been used to successfully model loss behavior in wired networks. Our goal here is to determine how well these models predict the first- and second-order frame-error statistics discussed in the previous section. Before describing these models, we first introduce some notation associated with Markov models.

We introduce a stochastic process $\{X_n, O_n\}_{n=0}^{\infty}$, where $\{X_n\}$ is a sequence of states associated with a finite state discrete time Markov chain that has transition probability matrix $A = [a_{ij}]$, and $\{O_n\}$ is a sequence of outputs generated by the Markov chain. In our context, $O_n \in \{0, 1\}$ and $n = 0, 1, \dots$, where 0 represents an error-free frame and 1 represents a corrupted frame. The statistics of O_n are described

as $P[O_n = 1|X_n = S_i] = b_i$ and $P[O_n = 0|X_n = S_i] = (1 - b_i)$; more specifically, a state, S_i , in the Markov process can output either 0 or 1, with a probability of outputting 1 as b_i .

Let us now briefly describe three discrete time Markov models. We begin with the k th-order Markov model as it is a component of the model proposed by Konrad et al.

3.1. k th-order Markov model

k th-order Markov models have been used to characterize packet loss in the Internet [13]. Since the states of a k th-order Markov model are observable, the transition probability matrix A is obtained by directly counting the frequencies of transitions occurring in the sample traces.

We define $S = \{0, 1\}^k$ to be the state space of a k th-order Markov process, where $s = s_1s_2 \cdots s_k \in S$ and $b_s = s_k$. Meanwhile, the transition from a state $s' = s'_1s'_2 \cdots s'_k$ to the state $s = s_1s_2 \cdots s_k$ occurs only if $s_j = s'_{j+1}$, where $j = 1, \dots, k - 1$. More precisely

$$P[X_{n+1} = s_1 \cdots s_k | X_n = s'_1 \cdots s'_k] = \begin{cases} a_{s's}, & s_j = s'_{j+1}, j = 1, \dots, k - 1; s_k = 1, \\ 1 - a_{s's}, & s_j = s'_{j+1}, j = 1, \dots, k - 1; s_k = 0, \\ 0, & s_j \neq s'_{j+1}, j = 1, \dots, k - 1. \end{cases} \quad (6)$$

Thus, deriving the transition matrix A of a k th-order Markov model from a loss sequence is based on counting the number of transitions from subsequence s' to subsequence s . We define the number of occurrence of subsequence s as n_s , and the number of occurrence of subsequence s' followed by subsequence s as $n_{s's}$. Thereafter, the transition probability from state s' to state s is calculated as follows:

$$a_{s's} = \begin{cases} \frac{n_{s's}}{n_{s'}}, & n_{s's} > 0, \\ 0, & \text{otherwise.} \end{cases} \quad (7)$$

Note that when $k = 1$, the k th-order Markov model reduces to a two-state Markov model. Since a k th-order Markov model needs 2^k states, the value for k is usually chosen to be small (typical values for k are 2–6).

3.2. MTA model

Konrad et al. [5] proposed a MTA algorithm. The MTA algorithm is as follows. The frame-error trace is divided into *lossy periods* and *loss-free periods*. A lossy period starts with an error frame, and terminates after C consecutive correctly received frames. Here, C is the sum of the mean and the standard deviation of error-frame burst lengths. After the trace is divided into lossy and loss-free frame sequences using C , the lengths of these frame sequences are assumed to be geometric with the averages obtained from the trace. While in a loss-free period, the output can only be 0 (the frame contains no error). In a lossy period, the output is determined by the states of a k th-order Markov model. The lossy period sequences are concatenated, and the concatenated lossy period sequence is used to calculate a k th-order Markov model. To generate synthetic traces consisting of correct or corrupted frames, the MTA algorithm first determines the lengths of pairs of loss-free and lossy states according to the two geometric distributions. Frame sequences are then generated as follows—a sequence of 0's fills in the error-free period, and a sequence of 0's and 1's, generated by the k th-order Markov model, is used to fill in the lossy period.

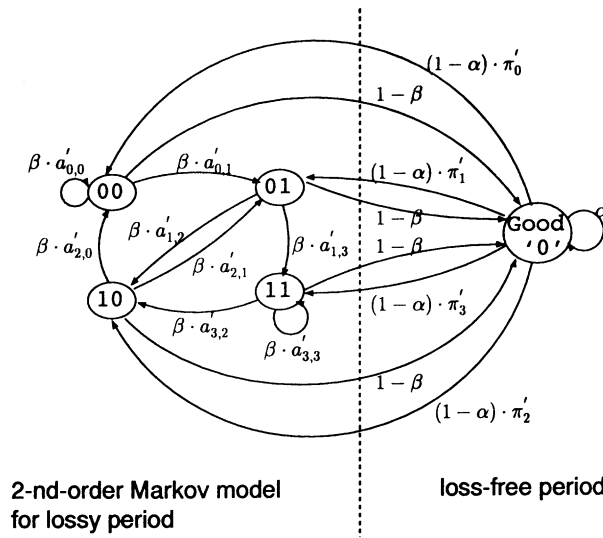


Fig. 5. Converting the MTA algorithm to a second-order MTA model.

A careful study of the MTA algorithm reveals that it is equivalent to a discrete time Markov model, where a k th-order Markov chain, as presented in Section 3.1, is used to model the concatenated lossy periods. In Fig. 5, we illustrate an example of the MTA algorithm with a second-order Markov model in the lossy period. In Fig. 5, a separate state is used to represent the loss-free period, where the transition probabilities for leaving or entering this special state ($1 - \alpha$ or $1 - \beta$, respectively) are derived from two geometric fittings of the lossy and loss-free period sequence lengths, and the transition probabilities among the lossy period states are derived from the concatenated lossy trace by using the scheme introduced in Section 3.1. Note that, in Fig. 5, a'_{ij} and π'_i are the transition probabilities and the stationary probabilities, respectively, of the k th-order Markov model only for the lossy period.

In this paper, for the convenience of comparison, we will refer to this model as k th-order MTA model, where k denotes the order of the high-order Markov model that is used to model the lossy period.

3.3. Hidden Markov models

HMMs [10], have recently been used to characterize Internet link losses [11], and have been found to better match certain statistics of the loss process than k th-order Markov models using the same number of states. In an HMM, the states and transitions between states are not observable. Each state can produce an output when it is visited, with the distribution of produced outputs being state-dependent. For example, for frame-error traces, the possible outputs of a state are either 1 or 0, with probabilities b_i and $1 - b_i$, respectively, and $0 \leq b_i \leq 1$. The EM algorithm, also known as the Baum–Welch algorithm, is used to estimate the parameters of the HMM that maximize the probability of outputting the observed sequence. Since the Baum–Welch algorithm is well described in many existing works, we omit its description in this paper. Interested readers can find descriptions of Baum–Welch algorithm and how a HMM is used to model a loss trace in [10,11].

In the next section, we will introduce the algorithms for calculating the first- and second-order statistics from a generic Markov model and compare the statistics derived from the three Markovian models introduced in this section with the statistics obtained from the empirical GSM frame-error trace.

4. Deriving the performance metrics from a Markov model

Let us now consider how well the performance measures predicted by the models match the measures found in the trace data. Two approaches are possible here: (i) use a model to generate synthetic traces and determine the measures from these traces; (ii) for our Markovian models, derive the performance measures directly from the model. In this paper, we use the second approach to evaluate the performance of different Markovian models. We use the notation introduced in Section 3.3. Note that, for a Markov model with observable states (e.g., the k th-order Markov model and the MTA model), $b_i = 1$ or 0 . However, for an HMM, $0 \leq b_i \leq 1$ for any state S_i :

- *FER*. We use the stationary distribution π to calculate the FER as

$$\text{FER} = \sum_{i=1}^N \pi_i b_i, \tag{8}$$

where N is the number of states.

- *Burst length distribution*. The CCDF of the burst lengths, either of 1's or 0's, is given by

$$F_{x^l}^{(c)}(x^l \geq n) = \frac{\pi(\mathbf{I} - B(l))(AB(l))^n \mathbf{1}}{\pi(\mathbf{I} - B(l))\mathbf{1}}, \quad l \in \{0, 1\}, \quad n \geq 1. \tag{9}$$

In Eq. (9), x^l represents the burst length of output l , π is the vector of the stationary probabilities, $\mathbf{1}$ the column matrix of ones, and $B(1) = \text{diag}\{b_i\}$, while $B(0) = \text{diag}\{1 - b_i\}$.

- *Autocorrelation function*. Alternative methods for calculating the autocorrelation functions from a Markov model can be found in [6,10–12]. Here, we present one method. We assume that the system is in steady state at time 0. The autocorrelation function of a Markov model is

$$\rho(\tau) = \frac{E[(O_0 - \mu)(O_\tau - \mu)]}{\mu^2}, \tag{10}$$

where τ is the lag, and μ the expectation of a model's output

$$\mu = \sum_{l \in \{0,1\}} l \pi B(l) \mathbf{1}. \tag{11}$$

Expanding Eq. (10), we obtain

$$\rho(\tau) = \frac{\sum_{O_0 \in \{0,1\}} \sum_{O_\tau \in \{0,1\}} (O_0 - \mu)(O_\tau - \mu) \text{Pr}[O_0, O_\tau]}{\mu^2}, \tag{12}$$

where the probability density of a Markov model generating output O_0 at time 0 and generating output O_τ at time τ is

$$\text{Pr}[O_0, O_\tau] = \pi B(O_0) A^\tau B(O_\tau) \mathbf{1}. \tag{13}$$

Thus, the autocorrelation function of a Markov model can be acquired.

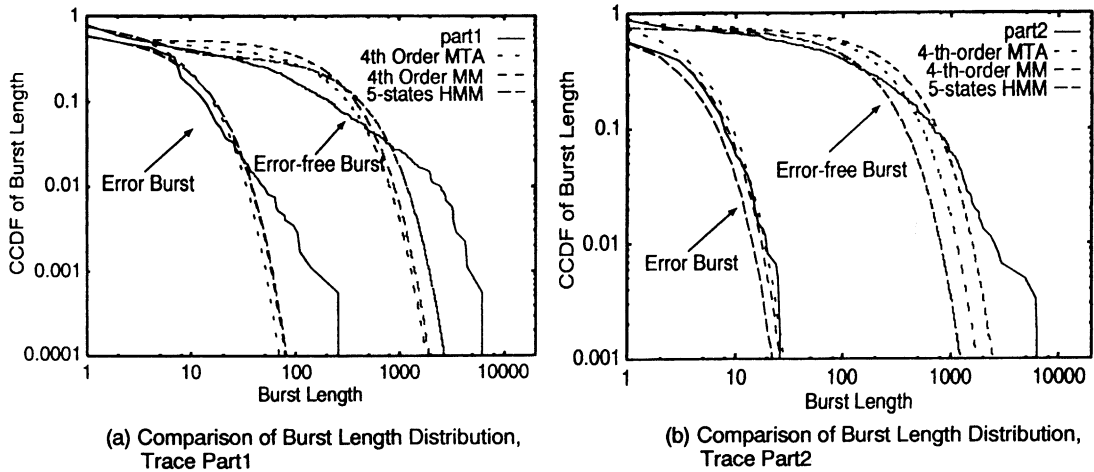


Fig. 6. Comparison of CCDF for error and error-free burst length of existing related models.

We now show the first- and second-order statistics derived from the three Markovian models that we presented, and compare them to the statistics of the empirical trace. Fig. 6 compares the burst length distributions of all three models to the burst length distributions of the empirical traces, part 1 (Fig. 6(a)) and part 2 (Fig. 6(b)) of the GSM channel. Fig. 7 compares their autocorrelations. For trace part 2, we observe that the fourth-order MTA model, fourth-order Markov model and five-states HMM all provide error burst length distributions reasonably close to original data trace. However with respect to the error-free burst length distribution, these models differ significantly from the original trace in their tail behavior. For trace part 1, these three models cannot capture the tail behavior of either the error burst or the error-free burst length distribution of empirical trace. In addition, we also observe that these models do not capture the autocorrelations of parts 1 and 2 well, as shown in Fig. 7. Finally, we note that, as shown in Table 2 of Section 5, the fourth-order MTA model does not predict the FER for either part 1 or 2 accurately, and the five-states HMM also does not accurately predict the FER for part 2 on average.

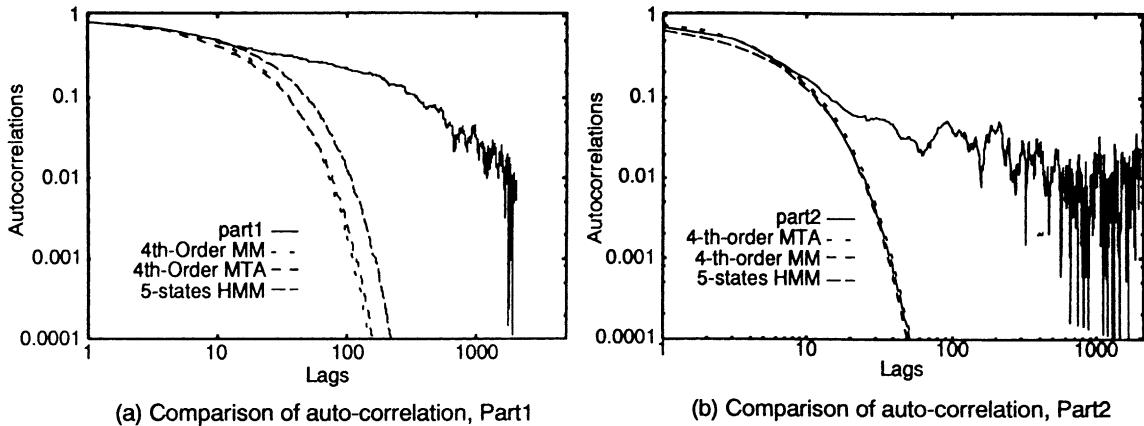


Fig. 7. Comparison of autocorrelation of existing related models.

Table 2
Prediction of FER

	FER	
	Part 1	Part 2
GSM trace	0.0503	0.0134
Fourth-order MTA	0.0663	0.0209
Fourth-order MM	0.0503	0.0139
Five-states HMM	0.0503 ± 0.0000	0.0140 ± 0.0060
Extended On/Off	0.0504	0.0134

These results suggest that existing models do not capture the tail behavior of the burst length distributions, the autocorrelation, or even the FER very well. In the next section, we use insights gained from our trace analysis to develop an extended On/Off model in order to more accurately reflect the variations in burst length.

5. The extended On/Off model

Recall from Section 2 our analysis of the empirical traces indicates that the error and error-free burst length distributions exhibit a greater variability than that of a geometric distribution. Furthermore, the trace exhibits significant temporal correlation. In the following subsection, we will observe that the successive loss and loss-free burst lengths are independent.

5.1. Cross-correlation of the error and error-free bursts

Let $\rho_c(h)$ be the sample correlation between the error and error-free burst length, with a lag h . We have

$$\rho_c(h) = \frac{1/(n-h) \sum_{i=1}^{n-h} (X_i - \bar{X})(Y_{i+h} - \bar{Y})}{\sigma_X \sigma_Y}, \quad (14)$$

where n is the number of sample bursts, $\{X_i\}$ and $\{Y_i\}$ are i.i.d. sequences of random variables corresponding to error and error-free burst lengths, with averages \bar{X} and \bar{Y} , and standard deviations σ_X and σ_Y , respectively. In Fig. 8, we show the cross-correlation, ρ_c , between error and error-free burst length of parts 1 and 2. The confidence bounds of ρ_c with significance level 0.05 are indicated as dashed lines in Fig. 8. From Fig. 8, we observe that the cross-correlation of error and error-free burst lengths is negligible for the GSM frame-error trace. This suggests that error burst lengths and error-free burst lengths are independent. In addition, we also studied the autocorrelations of the error and error-free burst lengths, and found negligible correlations within $\{X_i\}$ and $\{Y_i\}$. Thus, the frame-level error process might be well modeled by a discrete time two-state model in which frames are lost while the model is in an Off (error) state and not lost while the model is in an On (error-free) state. In order to capture the variability in the amount of time spent in each of these states, a mixture of geometric distributions is used. To avoid confusion, we will henceforth refer to a geometric distribution of the mixture of distributions as a geometric phase.

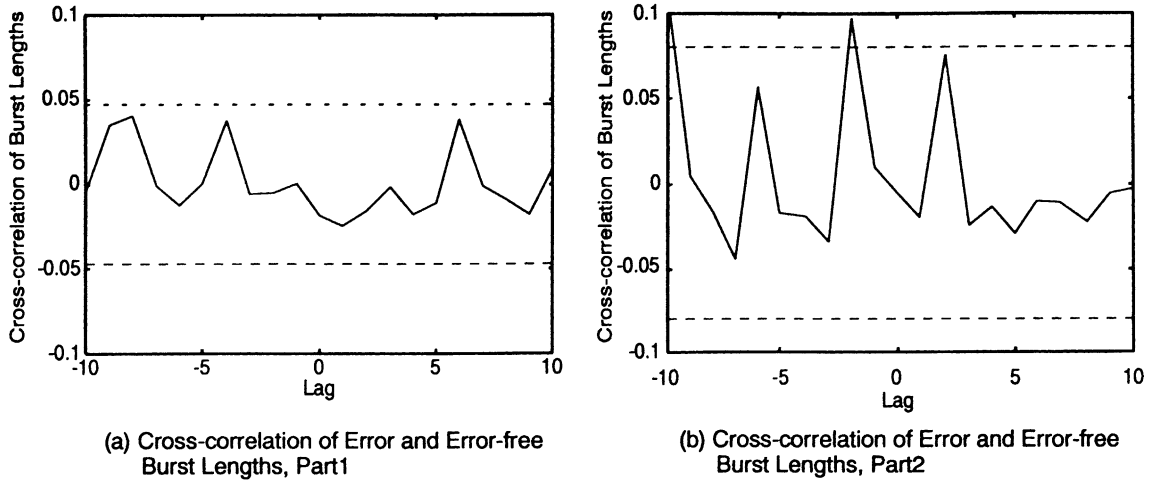


Fig. 8. Cross-correlation between error and error-free burst length of the GSM frame-error trace.

5.2. Fitting mixture geometric distributions to the On and Off-period

To obtain our extended On/Off model, we develop a scheme for fitting a mixture of geometric distributions to the burst length distributions of the On and Off-periods of the empirical frame-error trace. This technique is based on a previous work by Feldmann and Whitt [3] that presented a scheme for fitting a mixture of exponential distributions to a heavy-tail distribution.

The geometric distribution has the density function $P(X = x) = p^{x-1}(1 - p)$, and the cumulative distribution function (CDF), $P(X \leq x) = (1 - p)\sum_{i=1}^x p^{i-1} = 1 - p^x$. Therefore, a mixture of k geometric distributions has the following CCDF:

$$M(x) = \sum_{i=1}^k \alpha_i p_i^x, \tag{15}$$

where α_i ($1 \leq i \leq k$) denotes the weight parameter placed on the i th geometric phase. The parameters p_i in Eq. (15) are labeled so that $p_1 < p_2 < \dots < p_k$. Hence, the higher indexed components have tails which decay more rapidly. If p_2 is sufficiently larger than p_1 , then $\sum_{i=2}^k \alpha_i p_i^x$ should be negligible compared to $\alpha_1 p_1^x$ for x sufficiently large (in the tail). Similarly, when p_3 is sufficiently larger than p_2 , then $\sum_{i=3}^k \alpha_i p_i^x$ should be negligible compared to $\alpha_1 p_1^x + \alpha_2 p_2^x$ and so forth. Using this attribute, we fit the components of $M(x)$ recursively to the empirical data, starting with the pair (α_1, p_1) and then proceeding to the pair (α_2, p_2) and so on. In the rest of this paper, we denote the complementary length distribution of the On-period of the empirical trace as $F_0^{(c)}$, and the complementary length distribution of the Off-period of the empirical trace as $F_1^{(c)}$.

To perform the fitting, we first choose the number k of geometric phases used to fit the length distribution of the On or Off-period, as well as the k points at which we will match the empirical quantiles: $0 < x_k < x_{k-1} < x_{k-2} < \dots < x_1$. We assume that the ratios x_i/x_{i+1} are sufficiently large, e.g., we use $x_i = x_1 10^{-(i-1)}$ for $2 \leq i \leq k$. An example of how to define quantiles x_i is shown in Fig. 9. In Fig. 9, a mixture of three geometric distributions is chosen to fit the CCDF of the On-period burst length distribution. We

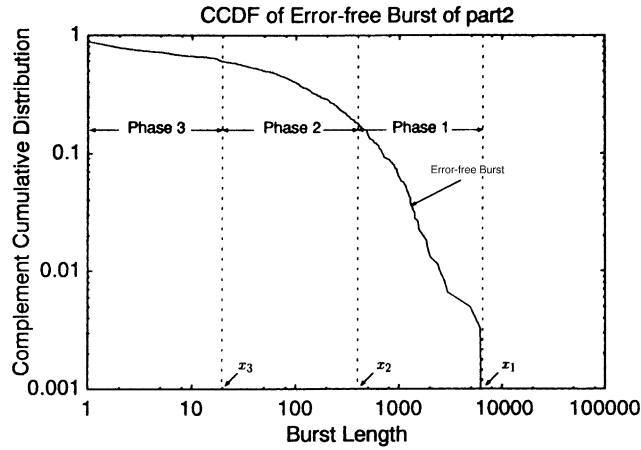


Fig. 9. An example of defining k (here, $k = 3$). Geometric phases for the error-free burst length.

assign x_1 to be the longest empirical burst length. Since there are two unknown parameters α_i and p_i for each phase, two empirical points are required to compute (α_i, p_i) . Let b be such that $1 < b < x_i/x_{i+1}$ for all i , e.g., with $x_i = x_1 10^{-(i-1)}$ we choose $b = 2$, and for each phase we choose the empirical quantiles x_i and x_i/b to perform the fitting. We fit the last phase first as follows:

$$F_0^{(c)}(x_1) = \alpha_1 p_1^{x_1}, \quad F_0^{(c)}\left(\frac{x_1}{b}\right) = \alpha_1 p_1^{x_1/b}. \tag{16}$$

For the other phases, we have

$$F_0^{(c)}(x_i) = \alpha_i p_i^{x_i} + \sum_{j=1}^{i-1} \alpha_j p_j^{x_i}, \quad F_0^{(c)}\left(\frac{x_i}{b}\right) = \alpha_i p_i^{x_i/b} + \sum_{j=1}^{i-1} \alpha_j p_j^{x_i/b}, \tag{17}$$

where (α_i, p_i) are the only two unknown parameters. We fit $M(x)$ to the On state and the Off state of the original frame-error trace separately, and thus get two mixtures of geometric distributions for the original trace. An extended On/Off model is shown in Fig. 10.

5.3. Using EM algorithm to estimate model parameters

We use the EM algorithm to improve the model parameters of our extended On/Off model. To initiate the EM algorithm, we first perform the fitting algorithm introduced in Section 5.2 on the GSM loss sequence.

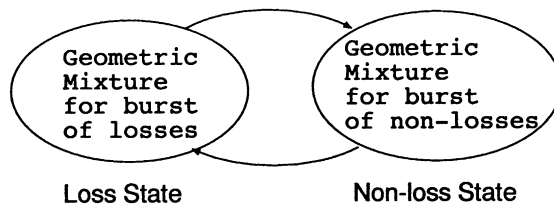


Fig. 10. An extended On/Off model.

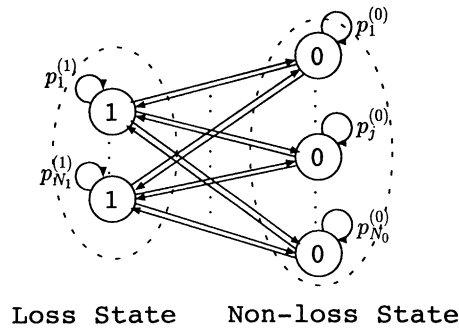


Fig. 11. The details of extended On/Off model.

More specifically, the extended On/Off model obtained by the fitting algorithm can be represented in the way shown in Fig. 11. Note that we assume that each state in the extended On/Off model has only one output, 1 for states in the Off-period and 0 for states in the On-period. No transitions occur between pairs of Off-period states or pairs of On-period states. We define the self-loop transition probability of an Off-period state as $p_i^{(1)}$, where $1 \leq i \leq N_1$, N_1 is the number of geometric phases for the Off-period; and the self-loop transition probability of an On-period state as $p_j^{(0)}$, where $1 \leq j \leq N_0$, N_0 is the number of geometric phases for the On-period. The transition probabilities $p_i^{(1)}$ and $p_j^{(0)}$ are obtained by fitting the mixture of geometric distributions to the burst length distributions of the loss and the loss-free period of the GSM empirical trace. We define the weight parameters obtained from the fitting algorithm for the Off-period as α_i ($1 \leq i \leq N_1$), and β_j ($1 \leq j \leq N_0$) for the On-period. Thus the transition probability from an Off geometric phase i to an On geometric phase j is initialized to be $(1 - p_i^{(1)})\beta_j$, and conversely $(1 - p_j^{(0)})\alpha_i$.

In this way, a generic On/Off model is acquired as shown in Fig. 11, where each state of the model is *observable* (being fixed to be either 1 or 0), yet the non-zero transition probabilities between states can be tuned. We then use the EM algorithm, particularly the Baum–Welch algorithm, to improve the model parameters for this extended On/Off model, so that the model exhibits a higher likelihood of generating the GSM empirical trace.

When tuning the model parameters based on the GSM empirical trace, we keep the state transition structures of the extended On/Off model unchanged as shown in Fig. 11. Since during the iterations of the Baum–Welch algorithm, the zero state transition probabilities and zero bi values remain the same, we directly employ Baum–Welch algorithm to fine tune the model parameters for our extended On/Off model. Our results show that the extended On/Off model with or without EM algorithm visually exhibits close performance on predicting the burst length distributions and the autocorrelation of the empirical trace parts (Fig. 12 shows the performance of part 2, while part 1 has similar results). However, the EM algorithm significantly improves the model’s capability of capturing the FER. Given these observations, in our later discussions, we only show the performance results of the model obtained after the EM algorithm is applied, and the *extended On/Off* model refers to the model utilizing EM algorithm.

To summarize, the state holding times of our extended On/Off model of the GSM channel are characterized by mixtures of geometric phases. The mixtures for each state are obtained by an algorithm that fits mixtures of geometric distributions to the On and Off-period. The EM algorithm is then used to fine tune the model parameters based on the initial extended On/Off model obtained by the fitting algorithm.

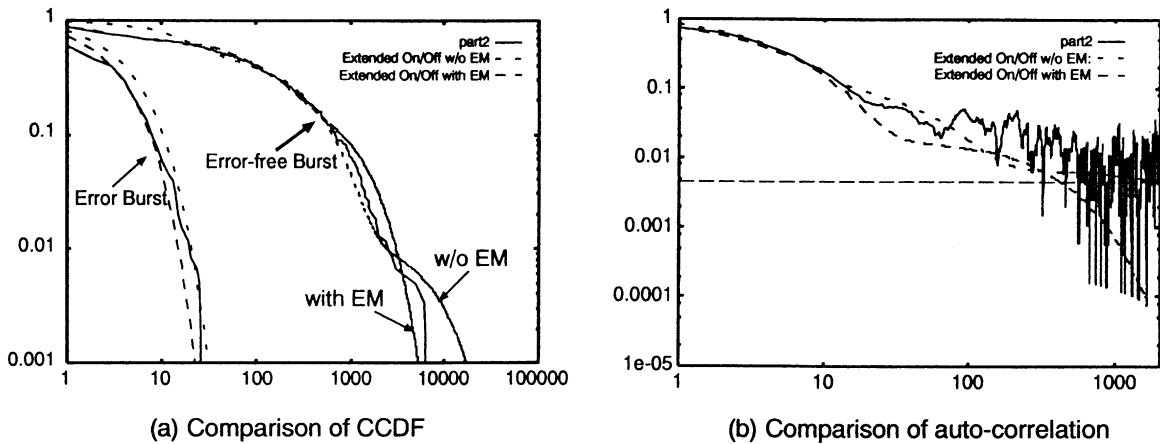


Fig. 12. Performance of the extended On/Off model with or without EM algorithm for part 2.

6. Evaluation results of the extended On/Off model

As in the previous section, we are interested in how well the performance measures predicted by the extended On/Off model match the measured observations in the empirical traces, and how the predictions of the extended On/Off model compare with those of the other models we described in the previous section.

In Table 2, we compare the predicted frame-error rates of all the models presented in this paper. For HMMs, the final HMM depends on the initial estimate of the parameters [10]. Thus, we computed 10 five-states HMM, and their corresponding FERs, and show the mean value and the errors of the FERs in Table 2. The extended On/Off model for part 1 has three geometric phases in the Off-period and four geometric phases in the On-period, and the extended On/Off model for part 2 has one geometric phase in the Off-period and three geometric phases in the On-period.

From Table 2, we observe that the extended On/Off model accurately captures the FER for both parts 1 and 2 of the GSM trace. The fourth-order MTA model, even with larger state space, fare less well. The fourth-order Markov model and the five-states HMM can predict FER for part 1 accurately; yet for part 2, neither of them performs as well as the extended On/Off model. Note that although the HMM considered in Table 2 has only five-states, the complexity of computing its parameters is significantly greater than that of the extended On/Off model, since transitions and outputs in the latter are much more constrained.

We also computed the CCDF and the autocorrelation of the extended On/Off model, and compared these with those of other models discussed. From our earlier Figs. 6 and 7, we know that the fourth-order MTA model, fourth-order Markov model, and the five-states HMM produce similar burst length distributions and autocorrelations. Thus, we only compare the extended On/Off model with the fourth-order MTA model in Figs. 13 and 14. In Fig. 13, we show the CCDFs of error and error-free burst lengths derived from the fourth-order MTA model and the extended On/Off model, and compare them with the CCDF of the empirical traces. From Fig. 13, we observe that the extended On/Off model captures the tail behavior of the burst length distributions significantly better than the fourth-order MTA model. Fig. 14 shows the autocorrelations derived from these two models, and the autocorrelation of the empirical traces.

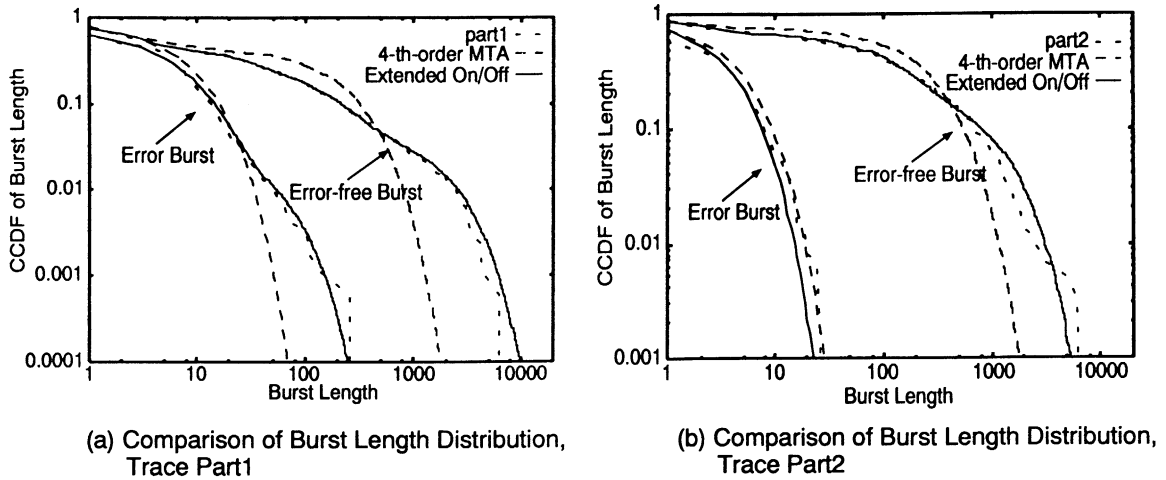


Fig. 13. Comparison of CCDFs for error and error-free burst length provided by the fourth-order MTA model and the extended On/Off model.

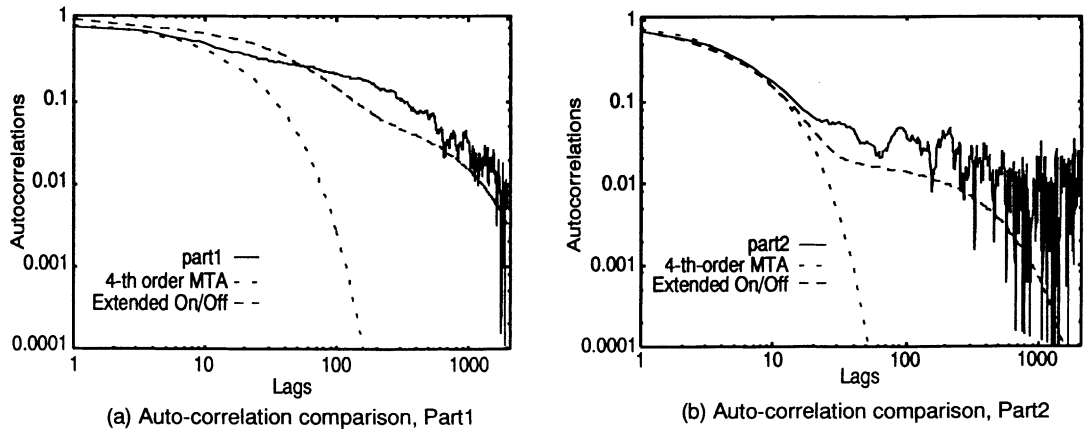


Fig. 14. Comparison of autocorrelations provided by the fourth-order MTA model and the extended On/Off model.

From Fig. 14, we observe that the extended On/Off model also predicts the autocorrelation much more accurately than the fourth-order MTA model (or other models with similar performance).

In addition, we also investigated the performance of extended On/Off model by varying the number of geometric phases that are used to capture the On or Off-period. Our results show that the performance of the extended On/Off model is not significantly improved by using more numbers of geometric phases.

7. Conclusion

In this paper, we have presented four different approaches towards modeling frame-level errors in GSM channels, including a new approach known as the extended On/Off model. We evaluated these approaches

against empirical GSM frame-level error traces and found that the extended On/Off model, with a small state space, captures both first- and second-order statistics significantly better than previously proposed approaches.

A lesson we learned through our work for modeling network traces is that a careful statistic analysis of the empirical data is necessary; it motivates appropriate modeling and analysis.

In our future work, we would like to apply mixtures of other distributions (e.g. Pareto, Lognormal, etc. [4]) for the On and Off states, and include the development and evaluation of models for frame-errors seen by mobile users.

References

- [1] J.S. Bendat, A.G. Piersol, *Random Data: Analysis and Measurement Procedures*, Wiley, New York, 1986.
- [2] P.J. Brockwell, R.A. Davis, *Introduction to Time Series and Forecasting*, Springer, Berlin, 1996.
- [3] A. Feldmann, W. Whitt, Fitting mixtures of exponentials to long-tail distributions to analyze network performance models, in: *Proceedings of INFOCOM*, vol. 3, 1997, pp. 1096–1104.
- [4] C. Jalpa-Villanueva, Z. Liu, N. Niclausse, S. Barbier, Web traffic characterization using mixture of parsimonious distributions, in: *Proceedings of the Symposium on Advanced Performance Modeling (SAPM)*, October 2000.
- [5] A. Konrad, B.Y. Zhao, A.D. Joseph, R. Ludwig, A Markov-based channel model algorithm for wireless networks, in: *Proceedings of the Fourth ACM International Workshop on Modeling, Analysis and Simulation of Wireless and Mobile Systems (MSWiM)*, 2001.
- [6] R.M.M. Leao, E. de Souza e Silva, S.C. de Lucena, A set of tools for traffic modeling analysis and experimentation, *Comput. Perform. Eval./TOOLS* 1786 (2000) 40–45.
- [7] M. Mouly, M.B. Pautet, *The GSM system for mobile communications*, 1992.
- [8] T.S. Rappaport, *Wireless Communications: Principle and Practice*, Prentice-Hall, Englewood Cliffs, NJ, 1996.
- [9] S. Ross, *Stochastic Processes*, Wiley, New York, 1996.
- [10] L.R. Rabiner, A tutorial on hidden Markov models and selected applications in speech recognition, *Proc. IEEE* 77 (2) (1989) 257–286.
- [11] K. Salamatian, S. Vaton, Hidden Markov modeling for network communication channels, in: *Proceedings of the ACM Sigmetrics*, 2001.
- [12] W. Turin, R. Van Nobelen, Hidden Markov modeling of flat fading channels, *IEEE J. Selected Areas Commun.* 16 (9) (1998).
- [13] M. Yajnik, S. Moon, J. Kurose, D. Towsley, Measurement and modelling of the temporal dependence in packet loss, in: *Proceedings of the IEEE INFOCOM*, New York, 1999.
- [14] M. Zorzi, R.R. Rao, Throughput performance of ARQ selective-repeat protocol with time diversity in Markov channels with unreliable feedback, *Wireless Networks* 2 (1996) 63–75.